Breathing gas calibration for MR $CMRO_2$ measurements: comparative effects on functional brain networks

D. Ivanov[1], G. Lohmann[1], S. Kabisch[1,2], I. Henseler[1], H. Schloegl[1,2], W. Heinke[3], C. Hutton[4], and R. Turner[1]
[1]Max Planck Institute for Human Cognitive and Brain Sciences, Leipzig, Germany, [2]Department of Medicine, University Hospital Leipzig, Leipzig, Germany, [3]Department of Anestesiology and Intensive Care Therapy, University Hospital Leipzig, Leipzig, Germany, [4]Wellcome Trust Centre for Neuroimaging, University College London, London, United Kingdom

Introduction: Regional changes in the cerebral metabolic rate of oxygen ($CMRO_2$) associated with neural activation can be estimated with MRI using the deoxyhaemoglobin (dHb) dilution model [1,2], which requires the calibration of resting-state blood oxygenation level dependent (BOLD) signal against an iso-metabolic change in the local dHb concentration. This change has mostly been achieved using hypercapnia, which elevates cerebral blood flow. Recently, hyperoxia has also been proposed as a calibration method [3,4]. A key assumption of the model is that the $CMRO_2$ in the area under study is not changed during the calibration step. Recently, there has been a debate about the influence of CO_2 on the global neural activity and global $CMRO_2$, with conflicting findings [5-8]. It is clear that CO_2 breathing influences some localized neural activity, and thus local $CMRO_2$, in regions associated with respiration control, provided there is a change in breathing [9]. In contrast, elevated oxygen concentration did not influence $CMRO_2$ in an anesthetized animal model [10]. Here we studied the effect of commonly used calibration gas mixtures on brain areas not previously investigated with calibrated functional MRI. For this purpose we assessed changes in functional connectivity (FC) networks using eigenvector centrality mapping (ECM) [11], a recently proposed model-free method for analysis of functional connectivity.

Materials and Methods: All experiments were performed on a 7 T whole-body MR scanner (MAGNETOM 7T, Siemens Healthcare Sector, Erlangen, Germany) using a 24-channel phased-array head coil (Nova Medical Inc, Wilmington MA, USA). The study was approved by the local ethics committee and all subjects gave informed consent. GRE EPI whole brain data were acquired from 12 healthy right-handed volunteers (3 male) with TR=2 sec, TE=25ms, and 3x3x3 mm^3 resolution. The subjects wore a nose clip, and air or a gas mixture was administered through a mouthpiece connected to a non-rebreathing gas delivery circuit throughout the course of the experiment. The gas mixtures were 50% O_2 and 50% N_2; 100% O_2; and 5% CO_2, 21% O_2 with 74% N_2. Each scanning session began with a 2 minute air breathing period followed by 4 minute long periods of breathing one of each gas mixture (in a randomized order across subjects) alternating with 4 minute long air breathing periods (total length = 26 minutes). The subjects were instructed to remain with their eyes open and try to breathe at a constant pace in order to avoid hyperventilation. The heart rate and the respiratory gas composition were recorded with a BIOPAC MP150 unit (BIOPAC Systems Inc, Goleta CA, USA) using a pulse oxymeter and sampling line connected to the mouthpiece. A physiological noise model was constructed to account for confounding effects of cardiac and respiratory phase, and end-tidal O_2 and CO_2 using a customized Matlab toolbox [12]. Models for cardiac and respiratory phase and their aliased harmonics were based on RETROICOR [13] and a similar, earlier method [14]. EPI data sets were corrected for differences in the slice acquisition times and head motion and transformed to Talairach space using LIPSIA[15]. The resulting physiological confounds and head motion parameters were regressed out of the BOLD data. Data sets lasting 100 seconds were selected for analysis from every breathing episode once the mean BOLD signal had reached a steady state after a change of the gas mixture (after more than 2 minutes). Finally, the data was smoothed with 6 mm 3D Gaussian kernel. For each subject and breathing episode, an eigenvector-centrality map (ECM) was created in the following way. First a correlation matrix was computed containing pairwise correlations between the fMRI time series at voxels within a manually defined mask covering the entire cerebrum (about 41,000 voxels). Next, the entries of the normalized eigenvector belonging to the largest eigenvalue of the correlation matrix are a measure of node centrality provided all entries in the matrix are positive. Note that negative entries in the matrix may lead to multiplicities of eigenvalues so that the largest eigenvector is only guaranteed to be uniquely defined after adding +1 to all correlation values (see Perron-Frobenius theorem). Voxels having high ECM value are highly correlated with many other voxels that are themselves well connected. Paired t-tests were used to compare the ECMs corresponding to the different breathing episodes, and Z-maps were generated. The statistical results were corrected for multiple comparisons using a Monte Carlo algorithm to simulate cluster size and peak values.

Results and Discussion: Figure 1 shows the difference between ECMs for the 50% oxygen breathing period compared with air breathing (thresholded at $p<0.05$, corrected for multiple comparisons) projected on three orthogonal cross-sections of a transparent brain derived from the average EPI brain volume. The areas with higher centrality (with color code for their Z-score) during the 50% O_2 breathing and air breathing are displayed in Fig. 1A and Fig. 1B, respectively. The highest Z-score (4.33) of the area in Fig. 1A has Talairach coordinates of [-2 -9 33] , which corresponds to middle cingulate cortex, an area reported to be involved in nonvolitional control of breathing [9]. The highest Z-score score in Fig. 1B (3.82) has Talairach coordinates of [34 42 18] which corresponds to dorso-lateral prefrontal cortex. The highest Z-score (3.69) of the other cluster of higher centrality in the air breathing phase has Talairach coordinates of [28 12 48]. There were no statistically significant differences between the 100% O_2 breathing phase and the air breathing phase. A possible reason for the disappearance of the regions observed in the difference between 50% O_2 and air breathing phases is that the cerebrospinal fluid in the cortical sulci becomes saturated with O_2 which shortens its T_1 value. In result, a MR signal increase unrelated to the underlying hemodynamic changes may mask and confound the observed BOLD fluctuations. Contrary to previous reports [7] we found no statistically significant difference between the 5% CO_2 and air breathing phase, even with almost identical preprocessing. This difference might stem from the fact that the approach we applied is model-free, i.e. it does not depend on a seed region or assumption about network validity to assess changes in connectivity.

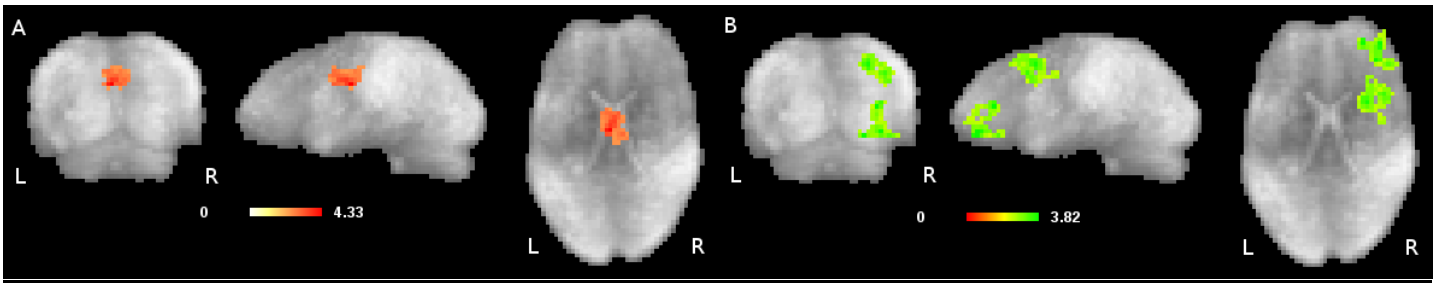

Figure 1: Eigenvector centrality difference maps for 50% O_2 vs air breathing (thresholded at $p<0.05$ corrected) projected on three orthogonal cross-sections of a transparent average brain with color-coded Z-scores. (A) Areas with statistically significant higher centrality in the 50% O_2 breathing phase. (B) Areas with statistically significant higher centrality in the air breathing phase.

Conclusion: The calibration methods studied, and mild hyperoxia with 50% O_2 in particular, seem to influence the brain functional connectivity only in limited regions which confirms their suitability for calibration of functional areas where $CMRO_2$ mapping has not been previously attempted.

References: [1] Davis TL et al, PNAS. 1998; [2] Hoge RD et al, Magn Reson Med. 1999; [3] Chiarelli PA et al, NeuroImage. 2007; [4] Mark CI et al, doi:10.1016/j.neuroimage.2010.08.070 [5] Zappe A et al, Cereb Cortex. 2008; [6] Chen JJ and Pike GB, J Cereb Blood Flow Metab. 2010; [7] Xu F et al, doi:10.1038/jcbfm.2010.153 [8] Bolar DS et al, Proc Intl Soc Mag Reson Med 2010; [9] McKay LC et al, NeuroImage. 2010; [10] Sicard K and Duong T, NeuroImage. 2005; [11] Lohmann G et al, PLoS One. 2010; [12] Hutton C et al, Proc Intl Soc Mag Reson Med 2010; [13] Glover GH et al, Magn Reson Med. 2000; [14] Josephs O et al, Proc Intl Soc Mag Reson Med 1997; [15] Lohmann G et al, Comput Med Imaging Graph 2001; [16] Zaharchuck G et al, Magn Reson Med. 2005;